



Optimization Study of Isolated Building using Shape Memory Alloy with Friction Pendulum System under Near-fault Excitations

D. Sreeman, B. Kumar Roy*

Department of Civil engineering, National Institute of Technology Silchar, India

PAPER INFO

Paper history:

Received 01 July 2022

Received in revised form 04 August 2022

Accepted 08 August 2022

Keywords:

Near-fault Earthquake
Friction Pendulum System
Base Isolation
Shape Memory Alloy

ABSTRACT

Structures close to causative earthquake faults may exhibit substantially different seismic responses than those recorded away from the excitation source. In the near-fault zone, long duration intense velocity pulses can induce unexpected seismic demands on isolated buildings. This study investigates the performance of a five-storey building frame isolated with a shape memory alloy based friction pendulum system (SMA-FPS) under near-fault excitations. The effectiveness of SMA-FPS is quantified by comparing the same isolated structure subjected to a friction pendulum system (FPS). Parametric studies, optimal analysis and numerical simulations are carried out on the structural parameters of the isolation systems. For this, the particle swarm optimization (PSO) method is used to acquire optimal characteristic strengths of SMA-FPS. The transformation strength of SMA and frictional coefficient are selected as two design variables to minimize the top storey acceleration, which is used as the objective function to optimize the seismic reduction efficiency of SMA-FPS system. The optimal seismic response of the structure isolated by SMA-FPS achieves superior performance over FPS under near-fault excitations. Moreover, the study reveals that the optimal SMA-FPS system significantly reduces the bearing displacement as compared to the FPS system. Finally, the computational results are validated with numerical simulation performed in SAP2000 which provides the consistent result.

doi: 10.5829/ije.2022.35.11b.12

1. INTRODUCTION

Passive vibration control systems of civil engineering structures such as tuned mass dampers [1-2] energy dissipation systems [3] and base isolation [4] systems are the most widely used structural vibration control techniques implemented in seismic prone areas to mitigate the detrimental effects of seismic excitations. The uses of passive, active, semi-active dampers and their effectiveness in vibration control systems for wind turbines, bridges and buildings were studied [5]. Among them, the base isolation (BI) system is one of the most effective vibration control methods which decouple the structure from earthquake ground motions. BI system by virtue of lower lateral stiffness shifts the fundamental time period of structure much higher and provides

additional structural damping. Many investigations [6,7] proved that the BI could mitigate the seismic response of the structural systems, and minimum energy is transferred to the superstructure [8]. Among the most common isolators, FPS has become a popular approach for retrofitting structures, industrial buildings and bridges due to its remarkable features. The FPS bearings consist of an articulated slider rested on concave surface [9]. The unique characteristic of the FPS is that in the presence of friction, the system acts like pendulum motion, and it can mitigate a large amount of energy through sliding and recenter by itself. In case of seismic activity, the spherical surface also provides a dynamic friction force that acts as a damping mechanism [10]. The horizontal displacement considerably minimizes the forces transmitted to the building even during large magnitude ground motions.

*Corresponding Author Institutional Email: bijan@civil.nits.ac.in
(B. Kumar Roy)

However, optimization technologies have been employed to design isolators with the optimal seismic behaviour [11]. Bucher [12] proposed a Pareto-type optimization technique to maximize the behaviour of FPS considering competing objectives related to the radius of curvature and frictional coefficient. To reduce the dynamic response of superstructure in aspects of displacement, the optimal ranges of coefficient of friction have been derived as a function of system parameters with different soil conditions [13]. Ozturk [14] proposed seismic drift assessment of structures in near-fault (NF) region. Numerous investigations have been conducted to examine an optimum design of FPS bearings under NF excitations [15]. NF ground motion records differ significantly from far fault (FF) earthquake records, where the engineering site distance is not more than 20 kilometres away from the fault rupture. NF seismic excitations contain long period velocity pulse in the normal fault direction, which stems from a permanent static offset of the ground [16]. NF ground motions might produce considerable ductility demands on FPS based structures, particularly at lower levels and it has also been shown that the pulse duration of seismic excitations substantially impacts the building's behaviour [17].

The study on NF excitations has become a research interest because of its sudden large impulse type of ground motion experienced by the structures. However, as seismic isolation technology advanced, the effectiveness of conventional isolators has been questioned in certain scenarios. Significantly, the behaviour of classical isolators under NF excitations has aroused severe concerns. Even though installing an isolation system reduces the building's response significantly, the velocity pulse found in NF excitations may induce amplification in the structural response of such long period buildings [18]. According to earlier investigations, a significant impact occurs when the slider of the FPS bearings is obstructed by the restrainer rims, resulting in severe damages such as the uplift of the isolator and detachment of isolator elements [19]. When structures using FPS systems are subjected to NF seismic excitations, the isolation level exhibits substantial deformations [20]. To address this issue, shape memory alloys (SMA) have been proposed as supplemental smart materials to reduce significant isolator displacement by mitigating the input earthquake forces [21]. SMA are alloys with significant damping properties, considerable dissipation of energy and has the ability to restore its original shape after large deformations [22]. SMAs significantly decrease the response of a structure since they are very effective energy absorbers and do not transmit energy from fundamental to higher vibration modes [23]. An overview of SMA with an isolation system and its prospective advantages in vibration techniques is studied [24]. Several efforts have been made to develop an SMA restrainer coupled with a

sliding type BI system to mitigate the bearing displacement [25]. Gur et al. [26] developed and designed a stochastic optimization method with two competing objectives and concluded that the combination of transformation strength of SMA and coefficient of friction mitigates the acceleration at floors and improves its isolation efficiency. The significant improvement of the SMA based rubber isolator over the elastomeric isolator for the isolated structure under NF motions was investigated [27]. An adaptive isolation system developed using an SMA based gap damper and low friction sliding surfaces is intended to mitigate significant deformations in the isolation system by introducing supplementary energy dissipation unless the deformations reaches a threshold value [28].

Although there have been several studies on the dynamic behaviour of FPS isolated buildings, limited studies have been done with SMA based LRB isolated buildings under NF seismic excitations. However, the influence of the building's response to NF excitations is not explored to the best of authors' knowledge using SMA-FPS system. A comparative study of the SMA-FPS isolation system with the FPS isolation system is performed to validate the efficiency of the SMA-FPS system on the seismic response of the building. In the parametric study, top storey acceleration and displacement in the isolator are used to measure the response quantities for this work. It is observed that there are some specific values of F_{so} and frictional coefficient that minimize the superstructure's acceleration and improve its isolation efficiency. Therefore, the parameters in SMA-FPS such as F_{so} and frictional coefficient are taken as design variables for performing particle swarm optimization of top storey acceleration as an objective function. The optimum values and corresponding design variables of SMA-FPS system are compared with the FPS system under the considered ground motions. Further, the results obtained from MATLAB 2D model are compared with the ones obtained in SAP2000 software package 3D model under NF earthquake ground motions.

2. RESPONSE EVALUATION OF SMA-FPS ISOLATED BUILDING USING NF GROUND MOTION

Figures 1(a) and 1(b) depict an N-storey shear-type building incorporated on the SMA-FPS and FPS isolator and their mechanical models, respectively. As the base isolation system significantly reduces the building's response, the superstructure behaviour may be considered linear. The lateral displacement is considered as degree of freedom for isolator mass and at each storey of a building. In matrix form, the dynamic equation of motion of an N-storey superstructure subjected to seismic input \ddot{z}_g is given as follows:

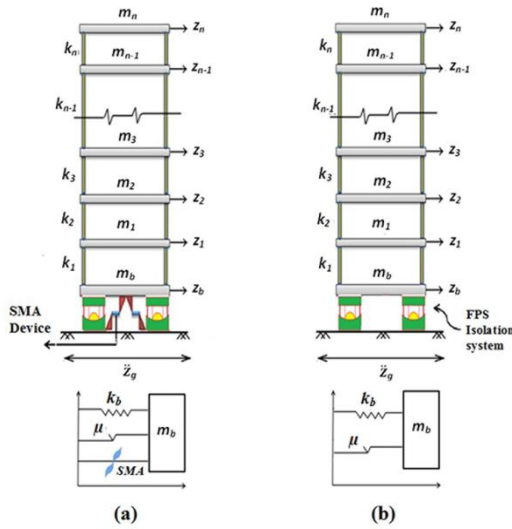


Figure 1. a) Flexible building and mechanical model with SMA-FPS b) Flexible building and mechanical model with FPS

$$[M]\{\ddot{z}\} + [C]\{\dot{z}\} + [K]\{z\} = -[M]\{r\}(\ddot{z}_g + \ddot{z}_b) \quad (1)$$

where $[M], [C]$ and $[K]$ are the matrices of size $N \times N$ indicating the superstructure's mass, damping and stiffness, respectively. Here $\{z\} = \{z_1, z_2, z_3, \dots, z_n\}^T$ represents the displacement vector that containing each storey's lateral displacement with respect to isolator. \ddot{z}_g is the acceleration of earthquake excitation. \ddot{z}_b is the isolator mass acceleration corresponding to its ground mass.

The generalized equation of motion of isolator mass is given as follows:

$$m_b \ddot{z}_b + F_b - c_1 \dot{z}_1 - k_1 z_1 = -m_b \ddot{z}_g \quad (2)$$

where m_b is the isolator mass, c_1 and k_1 represent the damping and stiffness of the first storey building, respectively; F_b is the isolator's restoring force. The term F_b in two different isolation systems is expressed as follows:

$$F_b(z_b, \dot{z}_b) = \begin{cases} k_b z_b + F_x & \text{for FPS Isolator} \\ k_b z_b + F_x + F_{SMA} & \text{for SMA-FPS Isolator} \end{cases} \quad (3)$$

The element $k_b z_b$ in Equation (3) represents restoring force of the bearings, where $k_b = \frac{W}{R}$ and $W = Mg$ represents weight supported by the bearings, g represents acceleration due to gravity and $M = \left(m_b + \sum_{i=1}^n m_i\right)$ indicates

system's total mass. The element F_x in Equation (3) denotes the friction force (F_x) generated at the sliding interface, which is calculated using the viscoplasticity model and expressed as $F_x = \mu WZ$. Where μ indicates FPS's frictional sliding coefficient and Z is a non-dimensional parameter considering $Z = \text{sgn}(\dot{z}_b)$, where $\text{sgn}(\cdot)$ is the signum function [29]. The signum function is equivalent to +1 or -1 based on whether \dot{z}_b is positive or negative, respectively. F_{SMA} is the SMA's restoring force. However, the functioning of the bearing system is nonlinear because a reversible phase transition of SMA induced by cycle loading-unloading, which dissipates the energy, as shown in Figure 2. A SMA alloy comes in variety of forms, including Nickel-Titanium (Ni-Ti) alloys, Cu alloys, Fe-Mn-Si alloys etc. Among them Ni-Ti alloys are frequently used in for seismic applications [30], which is considered in this study. For analysing the dynamic behaviour of SMA based structures, the Graesser-Cozarelli model [31] has been widely used. The system depends on the generic Bouc-wen model [32], with an additional component to account for super-elasticity effects and expressed as follows:

$$\dot{F}_{SMA} = k_s \left[\dot{z}_s - |\dot{z}_s| \left| \frac{\dot{F}_{SMA} - \beta}{F_{TS}} \right|^{\eta-1} \left(\frac{\dot{F}_{SMA} - \beta}{F_{TS}} \right) \right] \quad (4)$$

$$\beta = k_s \alpha_s \left[z_s - \frac{F_{SMA}}{k_s} + f_i |z|^c \text{erf}(a' z_s) \right] \quad (5)$$

in which β is the one-dimensional back stress expressed in Equation (5). The term k_s and z_s are the initial stiffness and displacement of the SMA, u_y is the yield displacement of SMA, α_s is a constant that defines the ratio of pre (OA) to post yield (AB) stiffness. F_{TS} is the force that initiates the phase transition from austenite to martensite. The yield transformation strength of SMA is easily normalized to the total weight of the structure

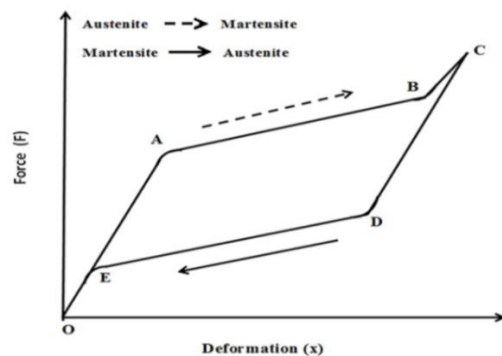


Figure 2. Hysteresis behaviour of shape memory alloy

(F_{so}). The term f_t is a constant, which controls the deformation loops. c' represents the slope of the unloading path (DE). η governs the sharpness of forward and backward transformation. The amount of recovery from unloading is governed by the constant a' . $|z_s|$ is the absolute value of z_s and dot over a variable indicates its time derivative. $erf(z_s)$ is the error function with an argument z_s , given as:

$$erf(z_s) = \frac{2}{\sqrt{\pi}} \int_0^{z_s} e^{-t^2} dt \quad (6)$$

By combining Equations (2) and (3), the resultant isolator equation given as follows:

$$m_b \ddot{z}_b + k_b z_b + F_x - c_1 \dot{z}_1 - k_1 z_1 = -m_b \ddot{z}_g \quad (7)$$

$$m_b \ddot{z}_b + k_b z_b + F_x + F_{SMA} - c_1 \dot{z}_1 - k_1 z_1 = -m_b \ddot{z}_g$$

The fundamental time period of SMA-FPS isolated system is expressed as $T_b = 2\pi \sqrt{\frac{M}{k_b + \alpha_s k_s}}$. The governing

equations for the behaviour of the superstructure-isolator system involve nonlinearity; therefore, the classical superposition technique cannot be applied. Furthermore, the isolation-superstructure system includes damping discrepancies, making the structure non-classically damped. Consequently, the governing Equations (1) and (7) are computed to determine the response of isolator and building by using Newmark's beta approach with a linear variation of acceleration and analyzed in MATLAB computer program.

3. NUMERICAL STUDY

A linear five storey shear building is considered in this study. Nonlinear dynamic analysis is used to evaluate the response of the SMA-FPS isolated building subjected to several NF real earthquake pulses. The parameters considered for this study are structural damping ratio (ξ_s), superstructure's time period (T_s) and taken as 2%, 0.5 seconds, respectively. For simplicity, the stiffness (k_i), mass (m_i) and the damping ratio of all the storeys are kept constant. The isolator mass to superstructure storey mass ratio ($\frac{m_b}{m}$) is taken as 1. For this analysis, the numerical values taken for the components to characterise the hysteretic behaviour of SMA-FPS and the FPS isolation system are provided in Table 1. The response parameters considered for evaluating the seismic behaviour of an isolated building are isolator displacement and top storey acceleration. For this

TABLE 1. Parameter values for SMA-FPS and FPS

Superstructure parameters	SMA-FPS/ FPS parameters	SMA parameters (Ni-Ti)
$\xi_s = 2\%$	$T_b = 2.5$ seconds $u_y = 0.025$ m	$\alpha_s = 0.10$, $f_T = 0.07$, $F_{so} = 0.10$
$T_s = 0.5$ seconds	$\mu = 0.05$	$\eta = 3$, $a' = 2500$, $c' = 0.001$

analysis, seven numbers of actual NF earthquake records are taken from PEER strong motion database with a wide range of broad spectrum and displacement amplitudes with relevant Peak ground acceleration (PGA), as shown in Table 2. The records selected are from earthquakes with magnitude (M_w) > 6.5.

The storey accelerations are considered as one of the essential seismic characteristics that are proportional to the external forces caused by the induced seismic activities. Figure 3(a) and (b) shows top storey acceleration and bearing displacement response of isolated building with SMA-FPS and FPS for NF ground motion (GM-1), respectively. Furthermore, NF records possess higher induced top storey acceleration and bearing displacement values. It has been observed that there is a superior performance of SMA-FPS over the FPS in mitigating the top storey acceleration and displacement in the isolator, especially under earthquakes with long period pulses encountered in the NF ground motions. Figure 4(a) and (b) depicts the hysteretic behaviour of an FPS and SMA-FPS bearings for NF ground motion, respectively. Hysteresis loops are

TABLE 2. Near-fault earthquake data

Sl. No.	Year	Earthquake	Station	M_w	PGA (g)
1.	1979	Imperial Valley (GM - 1)	El Centro array #5	6.53	0.38
2.	1979	Imperial Valley (GM - 2)	El Centro array #7	6.53	0.46
3.	1999	Chi-Chi (GM - 3)	TCU068	7.6	0.51
4.	1994	Northridge (GM - 4)	Rinaldi	6.7	0.87
5.	1994	Northridge (GM - 5)	Sylmar Converter	6.7	0.85
6.	1999	Kocaeli (GM - 6)	Duzce	7.5	0.40
7.	1999	Chi-Chi (GM - 7)	TCU067	7.6	0.49

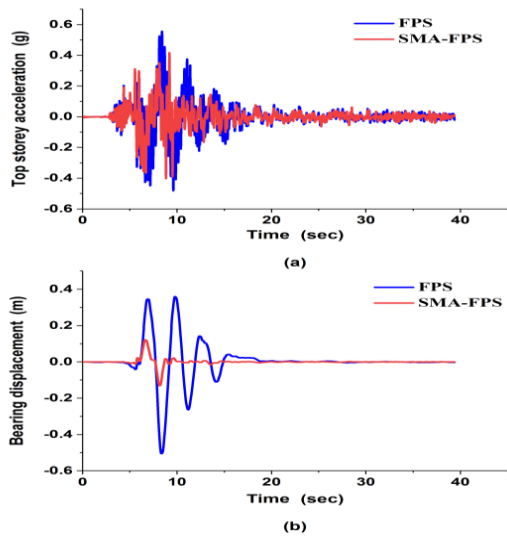


Figure 3. (a) Top storey acceleration (b) Bearing displacement of FPS and SMA-FPS isolated building against Imperial Valley ground motion (GM -1)

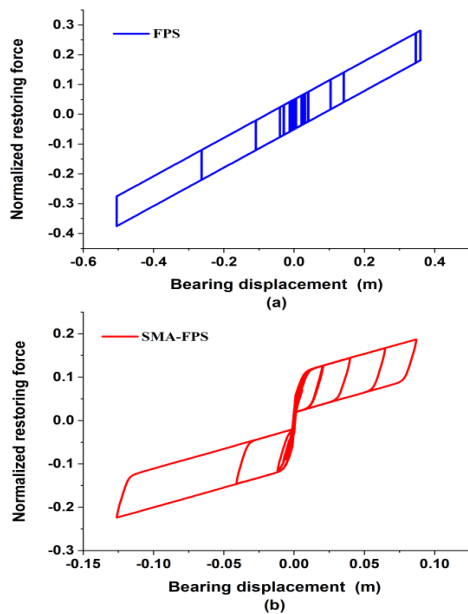


Figure 4. Hysteresis behaviour of FPS and SMAFPS isolated building under Imperial Valley ground motion (GM -1)

important for assessing the structural behaviour equipped with SMA-FPS and FPS isolators during seismic excitations. These hysteresis loops can extract and quantify seismic performance characteristics such as yield displacement, equivalent viscous damping, ductility, elastic and secant stiffness, ultimate displacement, ultimate load and yield load. It is observed that the hysteretic behaviour of SMA-FPS is fatter than FPS, hence SMA-FPS has better dissipation of energy than FPS system. However, additional dissipation of

energy in the SMA wires gives superior control efficiency in the SMA-FPS isolation system, especially in view of minimal displacement in the isolator.

The coefficient of friction and F_{so} are two important elements that affect the force deformation mechanism of SMA-FPS, and the response parameters (i.e. maximum top storey acceleration and isolator displacement) are evaluated by varying these two parameters. The average responses are then evaluated by combining these individual responses are shown in the respective figures by the thick line.

The effect of frictional coefficient and F_{so} on the response of isolated building is shown in Figure 5 as a whole. It is observed that with the increase in F_{so} values, the top storey acceleration decreases initially and reaches a minimum (optimal) value of response with respect to F_{so} in the SMA-FPS system (Figure 5a), and the same phenomenon is observed with an increase in frictional coefficient values (Figure 5c). As the F_{so} and frictional coefficient values increases, the isolator displacement decreases (Figure 5b) and SMA device in FPS system mitigates the isolator displacement significantly (Figure 5d), increasing its isolation efficiency under different NF seismic excitations. The base isolation system gets away from its ideal behaviour by increasing the frictional coefficient and restricting the free mobility of the isolation at the base level. As a result, increasing the frictional coefficient increases the maximum seismic energy penetrating the superstructure. However, the action of the SMA restrainer in FPS also prohibits excessive sliding from enhancing the acceleration.

Therefore, SMA-FPS gives a feasible alternative to the FPS system under NF seismic excitations.

4. PARTICLE SWARM OPTIMIZATION

In 1995, Eberhart and Kennedy [33] initially developed PSO. This algorithm is widely utilised in engineering applications. This optimization technique is based on evolutionary computational intelligence and can obtain a convergent solution utilising fish schooling and bird flocking models. PSO is a collective local and global search algorithm that can identify the optimal solution with limited memory and processing power. One of the major benefits of PSO is its capacity to save prior solutions for comparison with new ones. It is also simple to use because just a few parameters must be specified or modified. Each swarm member is distinguished by two characteristics, namely position and velocity. These two parameters are then utilised to update their particles. For estimating the next particle velocity and position are given in Equations (8) and (9).

$$u_i^{j+1} = \omega u_i^j + c_1 rand_1(pbest_i - y_i^j) + c_2 rand_2(gbest - y_i^j) \quad (8)$$

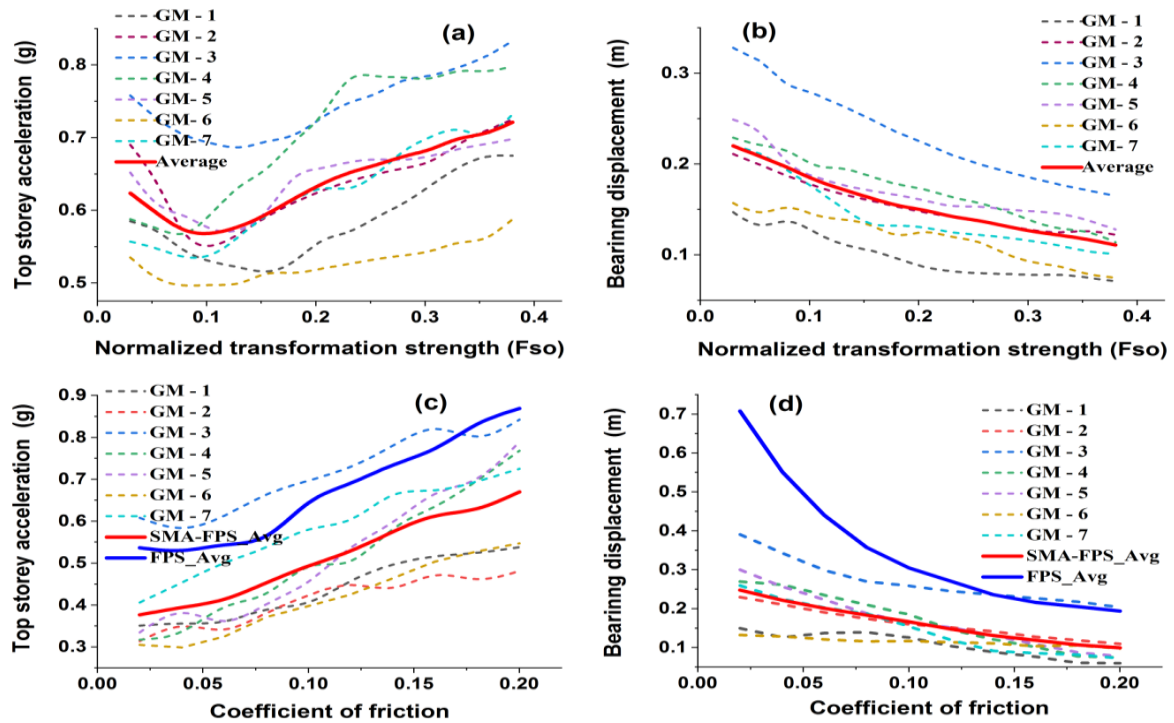


Figure 5. Variation of a) Top storey acceleration, (b) Isolator displacement against Fso of SMA-FPS and (c) Top storey acceleration, (d) Isolator displacement against coefficient of friction of FPS and SMA-FPS for all NF earthquake data

$$y_i^{j+1} = y_i^j + u_i^{j+1} \tag{9}$$

where $pbest$ is the particle’s best previous position and $gbest$ represents the position of the best particle up to that iteration in the entire swarm. c_1 and c_2 are the acceleration coefficients, $rand_1$ and $rand_2$ are two random numbers with a uniform distribution within the domain of $[0,1]$. ω denotes inertia weight factor that influences the impact of velocity memory on local and global search. The flow chart of PSO is shown in Figure 6.

5. PARAMETERS OPTIMIZATION OF SMA-FPS ISOLATION SYSTEM USING PSO

The building must remain operational even after a strong excitation to assist restoration efforts, thus optimal seismic design is required. Under these excitations, the SMA-FPS isolated building has some specific values of Fso and frictional coefficient that mitigate the structural accelerations and increases its isolation efficiency. For this, the PSO method is used to acquire optimal parameters (i.e., Fso and friction coefficient) of the SMA-FPS system. The relevant range for the design variables must be specified in the optimization

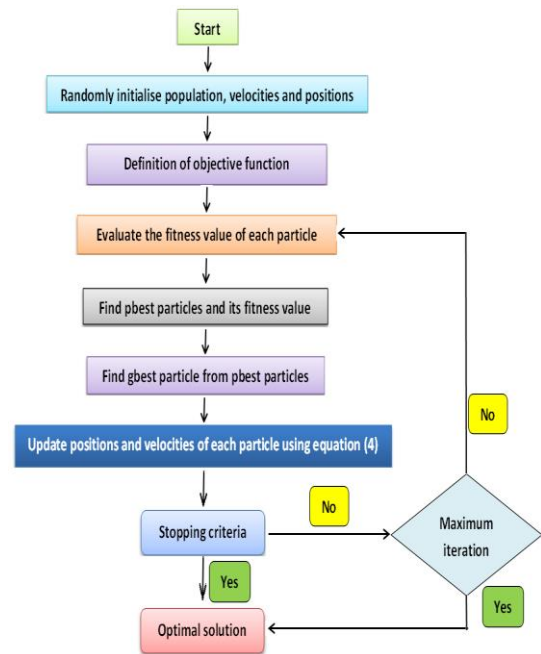


Figure 6. Flow chart of PSO algorithm for parameter identification

formulation. It is important to note that for both isolation systems, the objective function corresponds to the minimization of top storey superstructure accelerations.

The optimized top storey acceleration value and corresponding design variables such as F_{so} and frictional coefficients are obtained for different levels of the isolator time period, as depicted in Figure 7(a, b and c) as well as the associated bearing displacement of SMA-FPS and FPS isolation systems are depicted in Figure 7d for different NF seismic excitations. It can be found that the optimal parameter of F_{so} decreases with the increasing isolation time period, whereas the frictional resistance value increases. As the displacement related to SMA's phase transition remains constant for different levels of the time period of isolator. Consequently, lower stiffness values require increasing the isolation period, resulting in lower F_{so} values. Moreover, the frictional coefficient needs to be enhanced to avoid additional bearing displacement. Therefore, with an increase in time period of the isolator, the bearing displacement increases and the top storey acceleration reduces. Figures 8(a), 8(b) and 8(c) show the optimal top storey acceleration value and respective design variables, such as F_{so} and frictional coefficients, are obtained by varying superstructure flexibilities. Figure 8 (d) shows the corresponding bearing displacement of SMA-FPS and FPS isolation systems. The results found that, with an increase in superstructure flexibility, the optimal F_{so} and frictional resistance for the SMA-FPS system decreases because the coefficient of friction values should be lower to keep the isolation system efficient. The superiority of SMA-FPS over FPS in aspects of mitigating acceleration at top storey and large isolator displacements is further emphasized in Figures 8c and 8d. Although the top storey acceleration in the SMA-FPS system is typically lower

than that in the FPS system, the differences between them are not significant for various isolator and superstructure time periods (Figures 7c and 8c). However, SMA-FPS is more effective in minimizing the effects of significant bearing displacement.

6. NUMERICAL SIMULATION OF FPS ISOLATED BUILDING WITH SMA

In this section, the numerical analysis of isolated building with SMA-FPS is carried out and compared with the computational model for better reliability. The reinforced concrete building frame of five storeys has similar floor height of 3m each with three bays along shorter direction and four bays along longer direction of 3m width. To achieve the fundamental time period of building as 0.5 seconds, the elements and in both models (computational and numerical simulation) are adjusted accordingly. Two separate isolators namely FPS and SMA-FPS are modelled in SAP2000 software. In this work, SMA is modelled with the combination of two non-linear elements such as multi linear element elastic (MLE) and multi linear plastic (MLP) elements to simulate the superelastic and the force deformation behaviour of SMA wires. To model the SMA-FPS isolation system in software, the MLE, MLP link elements and friction isolator elements are arranged in parallel. Table 3 shows property of the multi linear elements that are employed in the softwares to portray FPS and SMA-FPS systems. A typical three dimensional RC building used for the purpose of numerical study is depicted in Figure 9.

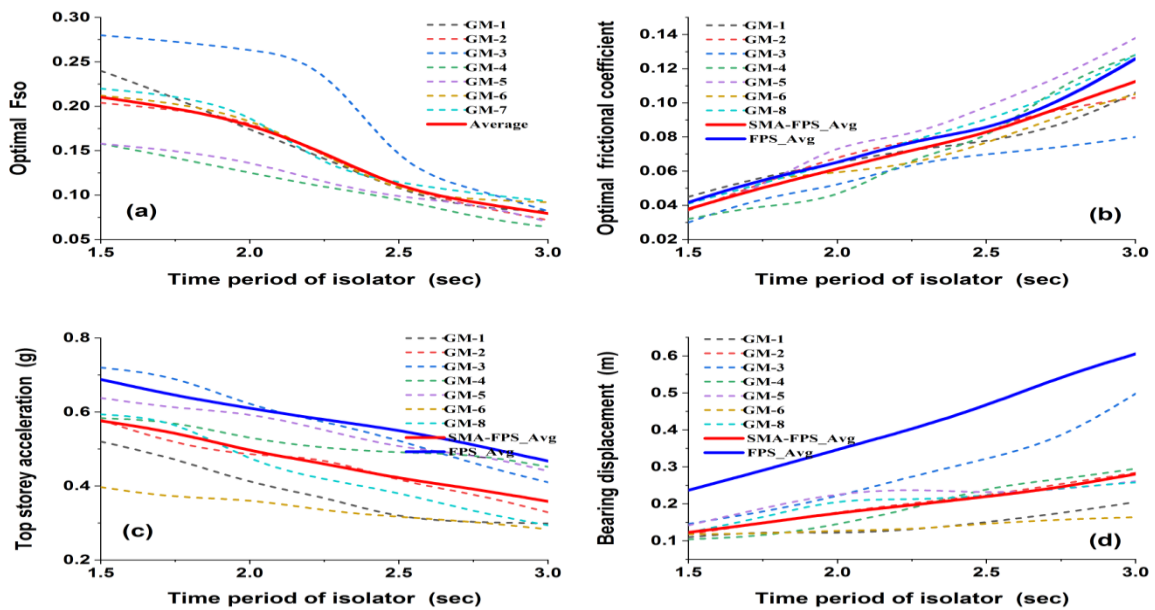


Figure 7. Optimum (a) F_{so} (b) coefficient of friction (c) top storey acceleration (d) bearing displacement against isolator time period for all NF earthquake data

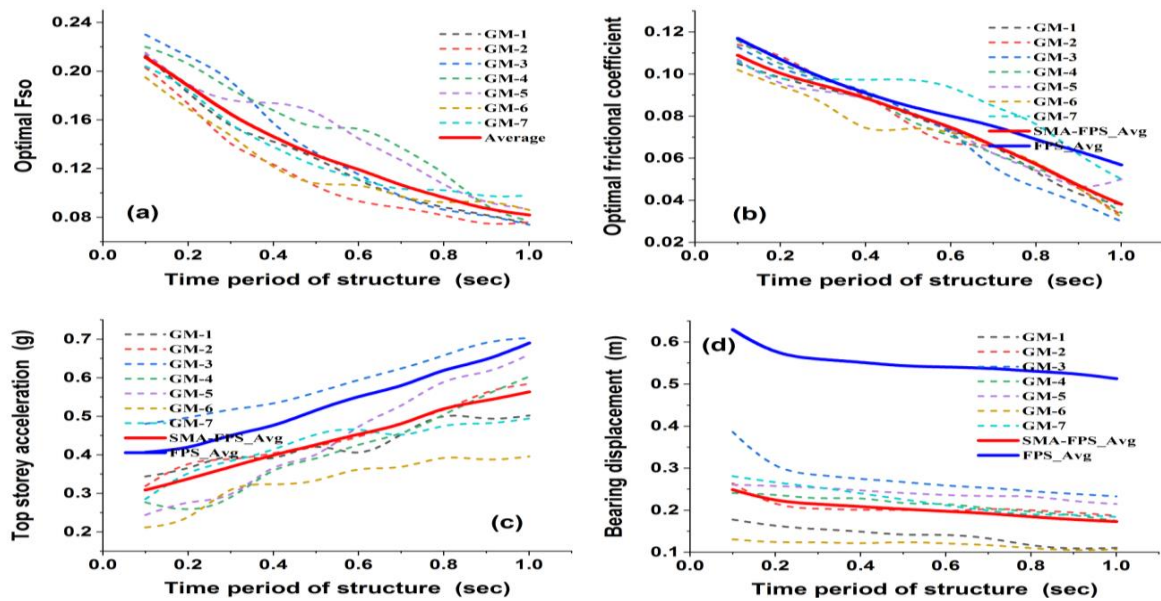


Figure 8. Optimum (a) Fso (b) coefficient of friction (c) top storey acceleration (d) bearing displacement against structural time period for all NF earthquake data

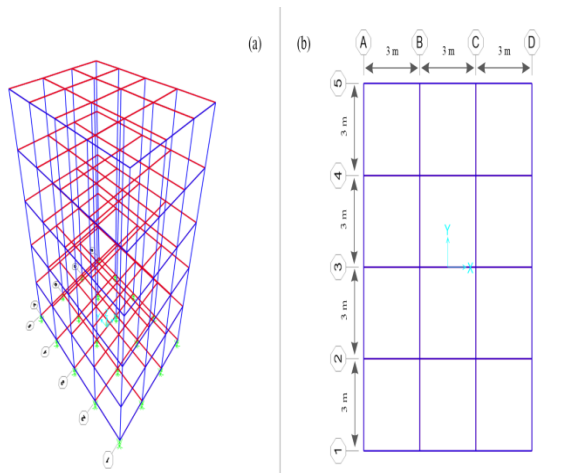


Figure 9. Building frame isolated with SMA-FPS (a) 3D view (b) Plan view

TABLE 3. Parameter values used in SAP2000

FPS parameters	Multi linear elastic	Multi linear plastic
K_v (vertical stiffness) = 170595 KN/m	Post yield stiffness ratio = 0.105	Yield exponent = 1 $\alpha = \infty, \beta = 0$
$K_{eff} = 720\text{KN/m}$ $R = 1.75\text{m}$	Yield displacement = 20mm	Yield displacement = 20mm

From the study, the comparison of computational and numerical results of top storey acceleration and bearing displacement response of isolated building with SMA-FPS and FPS isolation systems are shown in Figure 10

(a) and (b) respectively for GM-1 ground motion. The results obtained from the 3D model using SAP2000 are validated with those achieved from the computational results obtained in section 3. It can be mentioned here that in both the study similar trend of results are obtained for FPS and SMA-FPS isolation system. However, particular minor discrepancies are observed (from Table 4) among results which are approximately around 5% for top storey acceleration and 8% in case of bearing displacement for FPS and SMA-FPS base isolation systems respectively for computational and numerical model.

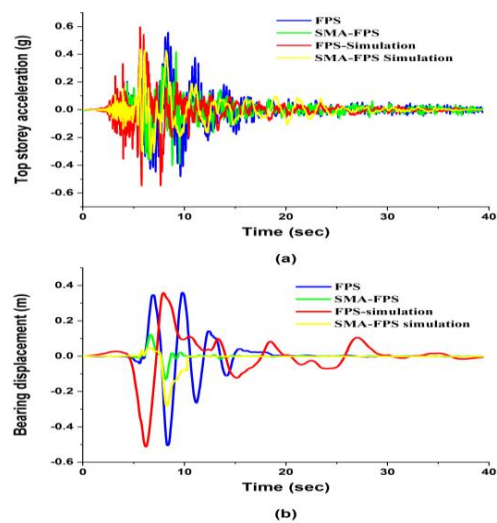


Figure 10. Comparison of a) Top storey acceleration b) Bearing displacement of computational and numerical simulation results

TABLE 4. Comparison of response parameters for computational and numerical model

Response parameters	Base isolators	Computational model	Numerical simulation	Error
Top storey acceleration (g)	FPS	0.552	0.581	4.99 %
	SMA-FPS	0.391	0.415	5.77%
Bearing displacement (m)	FPS	0.51	0.53	4.7%
	SMA-FPS	0.189	0.207	8.8 %

7. CONCLUSIONS

This study focuses on the effectiveness of SMA-FPS in mitigating the seismic response of isolated building under NF earthquakes. A parametric study and optimal analysis are carried out to determine the effect of SMA-FPS parameters on the responses of building and to investigate optimal parameters of the SMA-FPS isolation system using the PSO optimization technique. Comparative evaluation of SMA-FPS and FPS isolated building is conducted to emphasize its relative importance under the set of seven real earthquake ground motions. A parametric study reveals that the top storey acceleration and isolator displacement amplify significantly for the FPS isolation system subjected to NF pulses. However, the SMA-FPS isolation system mitigates the top storey acceleration and isolator displacement substantially compared to FPS isolation system. For structures subjected to NF seismic excitation, the SMA-FPS system can provide more effective energy dissipation than the FPS system. It is observed that there are some specific values of F_{so} and frictional coefficient that minimize the superstructure's top storey acceleration and improve its isolation efficiency. The F_{so} values decrease with increasing isolation time period as well as superstructure flexibilities, but the differences in optimal frictional coefficient remain relatively consistent for both isolation systems. Although the top storey acceleration in SMA-FPS system consistently lower than FPS system, but the differences between them are not significant for various isolator and superstructure time periods. However, the reductions in bearing displacement with increasing superstructure and isolator time periods are substantially reduced in SMA-FPS isolation system than FPS isolation system. Overall, by using SMA-FPS isolation system the response of the building can be improved over FPS system under the NF seismic ground motions. By comparing the response of the isolated structures modelled in numerical and computational methods, the results show a similar tendency in both the methods. However, there is a slight minor discrepancy in results obtained in numerical and computational methods, which proposed that the computational model can be used as a reliable study. However, the same study

can be performed by conducting hybrid experimental setup in future to validate the computational method.

8. REFERENCES

1. Pal, S., Roy, B., and Choudhury, S., "Comparative performance study of tuned liquid column ball damper for excessive liquid displacement on response reduction of structure", *International Journal of Engineering, Transactions B: Applications*, Vol. 33, No. 5, (2020), 753-759, doi: 10.5829/ije.2020.33.05b.06.
2. Ozturk, B., Cetin, H., and Aydin, E., "Optimum vertical location and design of multiple tuned mass dampers under seismic excitations", *Engineering Structures*, (2022), 1141-1163, doi: 10.1016/j.engstruct.2020.110536.
3. Barkhordari, M., and Tehranizadeh, M., "Ranking passive seismic control systems by their effectiveness in reducing responses of high-Rise buildings with concrete shear walls using multiple-Criteria decision making", *International Journal of Engineering, Transactions B: Applications*, Vol. 33, No. 8, (2020), 1479-1490, doi: 10.5829/ije.2020.33.08b.06.
4. Naeim, F., and Kelly, J. M., "Design of seismic isolated structures: from theory to practice", *John Wiley & Sons*, (1999), doi: 10.1002/9780470172742.
5. Basu, B., Bursi, O. S., Casciati, F., Casciati, S., Del Grosso, A. E., Domaneschi, M., Faravelli, L., Holnicki-Szulc, J., Irschik, H., and Krommer, M., "A European Association for the Control of Structures joint perspective. Recent studies in civil structural control across Europe", *Structural Control and Health Monitoring*, Vol. 21, No. 12, (2014), 1414-1436, doi: 10.1002/stc.1652.
6. Buckle, I. G., and Mayes, R. L., "Seismic isolation: history, application, and performance—a world view", *Earthquake Spectra*, Vol. 6, No. 2, (1990), 161-201, doi: 10.1193/1.1585564.
7. Jangid, R., and Kelly, J., "Base isolation for near-fault motions", *Earthquake Engineering & Structural Dynamics*, Vol. 30, No. 5, (2001), 691-707, doi: 10.1002/eqe.31.
8. Hessabi, R. M., Mercan, O., and Ozturk, B., "Exploring the effects of tuned mass dampers on the seismic performance of structures with nonlinear base isolation systems", *Earthquakes and Structures*, Vol. 12, No. 3, (2017), 285-296, doi: 10.12989/eas.2017.12.3.285.
9. Zayas, V. A., Low, S. S., and Mahin, S. A., "A simple pendulum technique for achieving seismic isolation", *Earthquake Spectra*, Vol. 6, No. 2, (1990), 317-333, doi: 10.1193/1.1585573.
10. Mokha, A., Constantinou, M., and Reinhorn, A., "Teflon bearings in base isolation I: Testing", *Journal of Structural Engineering*, Vol. 116, No. 2, (1990), 438-454, doi: 10.1061/(ASCE)0733-9445(1990)116:2(438).
11. Farzam, M. F., Jalali, H. H., Gavvani, S. A. M., Kayabekir, A. E., and Bekdaş, G., "Current trends in the optimization approaches for optimal structural control", *Advances in Structural Engineering-Optimization*, Vol. 326, (2021), 133-179, doi: 10.1007/978-3-030-61848-3-5.
12. Bucher, C., "Probability-based optimal design of friction-based seismic isolation devices", *Structural Safety*, Vol. 31, No. 6, (2009), 500-507, doi: 10.1016/j.strusafe.2009.06.009.
13. Castaldo, P., and Ripani, M., "Optimal design of friction pendulum system properties for isolated structures considering different soil conditions", *Soil Dynamics and Earthquake Engineering*, Vol. 90, (2016), 74-87, doi: 10.1016/j.solidyn.2016.08.025
14. Ozturk, B. M., "Seismic drift response of building structures in seismically active and near-fault regions", Purdue University, 2003.

15. Jangid, R, "Optimum friction pendulum system for near-fault motions", *Engineering Structures*, Vol. 27, No. 3, (2005), 349-359, doi: 10.1016/j.engstruct.2004.09.013.
16. Iwan, W. D, "Near-field considerations in specification of seismic design motions for structures" Proceedings of the Tenth European Conference on Earthquake Engineering, Vienna, Austria, August, (1994), 257-267.
17. Mazza, F, and Vulcano, A, "Effects of near-fault ground motions on the nonlinear dynamic response of base-isolated rc framed buildings", *Earthquake Engineering & Structural Dynamics*, Vol. 41, No. 2, (2012), 211-232, doi: 10.1002/eqe.1126.
18. Mazza, F., Vulcano, A, and Mazza, M, "Nonlinear dynamic response of RC buildings with different base isolation systems subjected to horizontal and vertical components of near-fault ground motions", *The Open Construction & Building Technology Journal*, Vol. 6, No. 1, (2012), doi: 10.2174/1874836801206010373.
19. Becker, T. C., Bao, Y, and Mahin, S. A, "Extreme behavior in a triple friction pendulum isolated frame", *Earthquake Engineering & Structural Dynamics*, Vol. 46, No. 15, (2017), 2683-2698, doi: 10.1002/eqe.2924.
20. Mazza, F, "Lateral-torsional response of base-isolated buildings with curved surface sliding system subjected to near-fault earthquakes", *Mechanical Systems and Signal Processing*, Vol. 92, (2017), 64-85, doi: 10.1016/j.ymsp.2017.01.025.
21. Ozbulut, O. E, and Hurllebaus, S, "Seismic assessment of bridge structures isolated by a shape memory alloy/rubber-based isolation system", *Smart Materials and Structures*, Vol. 20, No. 1, (2010), 015003, doi: 10.1008/0964-1726/20/1/015003.
22. Rouhbakhsh, D. A, and Sadmezah, S, "A 3d micro-plane model for shape memory alloys", *International Journal of Engineering, Transactions A: Basics*, Vol. 21, No. 1, (2008).
23. Casciati, F, and Faravelli, L, "A passive control device with SMA components: from the prototype to the model", *Structural Control and Health Monitoring*, Vol. 16, No. 7-8, (2009), 751-765, doi: 10.1002/stc.328.
24. Ozbulut, O. E., Hurllebaus, S, and DesRoches, R, "Seismic response control using shape memory alloys: a review", *Journal of Intelligent Material Systems and Structures*, Vol. 22, No. 14, (2011), 1531-1549, doi: 10.1177/1045389X11411220.
25. Ozbulut, O. E, and Hurllebaus, S, "A comparative study on the seismic performance of superelastic-friction base isolators against near-field earthquakes", *Earthquake Spectra*, Vol. 28, No. 3, (2012), 1147-1163, doi: 10.1193/1.4000070.
26. Gur, S, and Mishra, S. K, "Multi-objective stochastic-structural-optimization of shape-memory-alloy assisted pure-friction bearing for isolating building against random earthquakes", *Soil Dynamics and Earthquake Engineering*, Vol. 54, (2013), 1-16, doi: 10.1016/j.solidyn.2013.07.013.
27. Gur, S., Mishra, S. K, and Chakraborty, S, "Performance assessment of buildings isolated by shape-memory-alloy rubber bearing: comparison with elastomeric bearing under near-fault earthquakes", *Structural Control and Health Monitoring*, Vol. 21, No. 4, (2014), 449-465, doi: 10.1002/stc.1576.
28. De Domenico, D., Gandelli, E, and Quaglini, V, "Adaptive isolation system combining low-friction sliding pendulum bearings and SMA-based gap dampers", *Engineering Structures*, Vol. 212, (2020), 110536, doi: 10.1016/j.engstruct.2020.110536.
29. Castaldo, P., Palazzo, B, and Della Vecchia, P, "Seismic reliability of base-isolated structures with friction pendulum bearings", *Engineering Structures*, Vol. 95, (2015), 80-93, doi: 10.1016/j.engstruct.2015.03.53.
30. Dolce, M., Cardone, D, and Marnetto, R, "Implementation and testing of passive control devices based on shape memory alloys", *Earthquake Engineering & Structural Dynamics*, Vol. 29, No. 7, (2000), 945-968, doi: 10.1002/1096-9845(200007)29:7<945::AID-EQE958>3.0.
31. Graesser, E, and Cozzarelli, F, "Shape-memory alloys as new materials for aseismic isolation", *Journal of Engineering Mechanics*, Vol. 117, No. 11, (1991), 2590-2608, doi: 10.1061/(ASCE)0733-9399(1991)117:11(2590).
32. Wen, Y. K, "Equivalent linearization for hysteretic systems under random excitation", *Journal of Applied Mechanics*, Vol. 47, No. 1, (1980), 150-154, doi: 10.1115/1.3153594.
33. Eberhart, R, and Kennedy, J, "A new optimizer using particle swarm theory", MHS'95. Proceedings of the Sixth International Symposium on Micro Machine and Human Science, (1995), 39-43.

Persian Abstract

چکیده

سازه‌های نزدیک به گسل‌های زلزله‌ای ممکن است واکنش‌های لرزه‌ای متفاوتی نسبت به سازه‌هایی که دور از منبع تحریک ثبت شده‌اند نشان دهند. در ناحیه نزدیک به گسل، پالس‌های سرعت شدید طولانی مدت می‌توانند تقاضاهای لرزه‌ای غیرمنتظره‌ای را در ساختمان‌های جدا شده ایجاد کنند. این مطالعه عملکرد یک قاب ساختمان پنج طبقه ایزوله شده با سیستم آونگ اصطکاکی مبتنی بر آلیاژ حافظه شکل (SMA-FPS) را تحت تحریکات نزدیک به گسل بررسی می‌کند. اثربخشی SMA-FPS با مقایسه همان ساختار جدا شده تحت یک سیستم آونگ اصطکاکی (FPS) اندازه‌گیری می‌شود. مطالعات پارامتریک، تحلیل بهینه و شبیه‌سازی عددی بر روی پارامترهای ساختاری سیستم‌های جداسازی انجام می‌شود. برای این کار، از روش بهینه سازی ازدحام ذرات (PSO) برای به دست آوردن نقاط قوت مشخصه بهینه SMA-FPS استفاده می‌شود. قدرت تبدیل SMA و ضریب اصطکاک به عنوان دو متغیر طراحی برای به حداقل رساندن شتاب طبقه بالایی انتخاب شده‌اند که به عنوان تابع هدف برای بهینه‌سازی راندمان کاهش لرزه‌ای سیستم SMA-FPS استفاده می‌شود. پاسخ لرزه ای بهینه سازه ایزوله شده توسط SMA-FPS به عملکرد برتر نسبت به FPS تحت تحریکات نزدیک به گسل دست می‌یابد. علاوه بر این، این مطالعه نشان می‌دهد که سیستم بهینه SMA-FPS به طور قابل توجهی جایجایی بلبرینگ را در مقایسه با سیستم FPS کاهش می‌دهد. در نهایت، نتایج محاسباتی با شبیه‌سازی عددی انجام‌شده در SAP2000 اعتبارسنجی می‌شوند که نتیجه سازگار را فراهم می‌کند.
